

# Flow Separation Control of Backward-Facing Step Airfoil NACA0015 by Blowing Technique

Khuder N. Abed

*Department of Mechanical Engineering, College of Engineering, University of Diyala*  
Khuder@engineering.uodiyala.edu.iq

## Abstract

The aim of this paper is to control the flow separation above backward-facing step (BFS) airfoil type NACA 0015 by blowing method. The flow field over airfoil has been studied both experimentally and computationally. The study was divided into two parts: a practical study through which NACA 0015 type with a backward-facing step (located at 44.4%  $c$  from leading edge) on the upper surface containing blowing holes parallel to the airfoil chord was used. The tests were done over two-dimensional airfoil in an open circuit suction subsonic wind tunnel with flow velocity 25m/s to obtain the pressure distribution coefficients. A numerical study was done by using ANSYS Fluent software version 16.0 on three models of NACA 0015, the first one has backward-facing step without blowing, the second with single blowing holes and the third have multi blowing holes technique. Both studies (experimental and numerical) were done at low Reynolds number ( $Re=4.4 \times 10^5$ ) and all models have chord length 0.27m. The experimental investigations and CFD simulations have been performed on the same geometry dimensions, it has been observed that the flow separation on the airfoil can be delayed by using velocity blowing (30m/s) on the upper surface. The multi blowing holes with velocity improved the aerodynamics properties. The multi blowing holes and single blowing hole the same effect on pressure distribution coefficients.

**Keywords:** Flow Separation; Backward-Facing Step; Blowing Technique.

## Paper History:

(Received: 11/9/2017, Accepted: 7/1/2018)

## 1. Introduction

The field of flow separation control has a great interest and a progress search for refinement in high lift device performance seen has been explored. This progress occurs because of an improvement in understanding fluid mechanics and the progress reached in computational techniques, the experimental work availability and the existing of flow control mechanisms nowadays. These mechanisms effect active and passive flow control techniques. Flow control over airfoils is mainly forced to be increasing the

lift and decreasing the drag. Caused by the airfoil. This can be done by controlling the boundary and shear layer flows to reduce the separation region to the minimum over the suction surface of the airfoil [1, 2]. Saric et al. [3] studied computationally employ (LES) large eddy simulation, (DES) detached eddy simulation, and (T-RANS) transient Reynolds-averaged Navier–Stokes methods to limit turbulent flow above a backward-facing step (BFS) troubled at equal intervals by changing blowing/suction through a thin slit (0.05  $H$  width) mounted at the step edge. A troubled frequency  $St=0.19$  was used with a length decrease to 28.3% was compared to untroubled situation which has better agreement with computational methods. Uruba et al. [4] performed an experimental work of channel flow behind a backward-facing step by blowing/suction near the step. Blowing and suction were dominate causing reduction in the length of the separation zone down to one third of its value when no control in used. Two parameters are important for blowing (slot area and shape) in which small cross-section and serrated edge is the most operative. Interaction of the boundary layers near the edge of the step cause the three dimensions vortex structure near the crack to be existed. Mishriky et al [5] numerically investigate the introduction of a backward-facing step on the suction side of NACA 2412 airfoil at a high Reynolds number. To find the best position for the step, a study was done to know the position of the step on the lift coefficient, drag coefficient and critical angle of attack. Results showed that introducing such a suction side of NACA 2412 airfoil have on inversely effect on considerable properties.

Hasan et al [6] Investigate experimentally a flow over a backward-facing step with laminar separation under controlled perturbation ( $Re=11000$ ). The ‘shear layer mode’ and the ‘step mode’ was two distinct modes of instability found for the reattaching shear layer. The disturbance increased the rate of growth of the shear layer and the intensity of the turbulence and decreased the length of reattachment compared to the undisturbed flow. Flow visualization confirmed the division of the shear layer and showed the existence of a low-frequency flapping of the shear layer. Chun et al [7] investigate a backward-facing step Excitations to separate the flow using a sine

wave oscillatory jet to study flow over (BFS). A jet introduced from a slot near separation line. It is noticed an enhancement in shear layer grow the rate due to localized forced near the separation edge with small amount, which cause a roll-up vortex. Rise in higher rate of internment caused by large vortex in shear layer. Reduction in reattached length compered to unfree flow is noticed due to this parameter.

The goal of current research is to control the flow separation on the (BFS) airfoil type NACA 0015 by blowing method. The study was divided into two parts: a practical study on airfoil with (BFS) on the upper surface containing blowing holes placing parallel to the airfoil chord. The blowing system consists of a two-stage reciprocating air compressor used to compress air to the wings through the tube. The velocity of the air that was blowing was measured with a pitot-static tube. A numerical study using ANSYS Fluent software version 16.0 on three models of NACA 0015,

backward-facing step without blowing holes, with single blowing holes and with multi blowing holes technique.

## 2. Experimental Work

All experiments were made in an open circuit suction subsonic wind tunnel. The manufacturing of open wind tunnel (wide range of investigations into aerodynamics) by engineering technical college of Mosul. The tunnel has an open test section of 300mm by 300mm cross section and 500mm length. Maximum free stream wind velocity  $U_{\infty}$  is about 36 m/s, and the chord Reynolds number is about  $4.4 \times 10^5$ . The free stream is fixed at 25m/s for the present experiment. A rectangular wing with NACA 0015 airfoil (Wood with Aluminum) was used for the tests. Figure 1 shows the arrangement of the working section in wind tunnel.

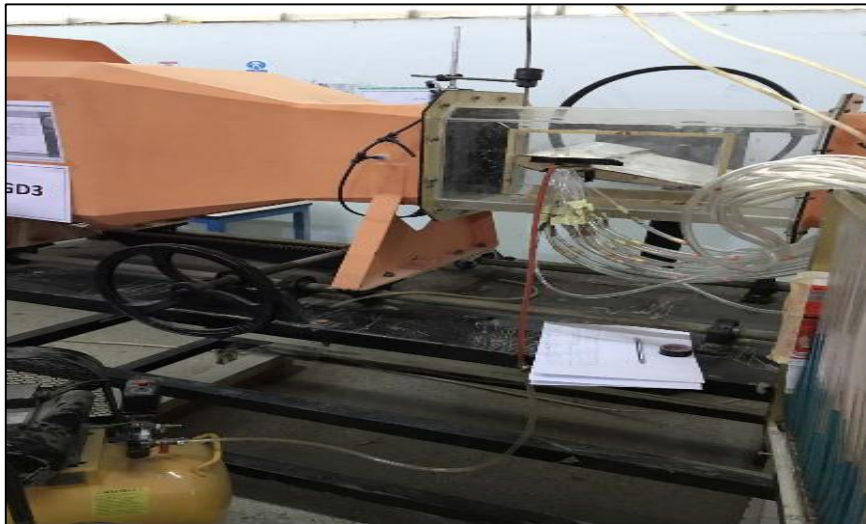


Figure 1: Backward-facing step (BFS) airfoil type NACA 0015 mounted inside wind tunnel with blowing method

Wing chord was 270 mm; wingspan 297 mm and the angle of attack  $\alpha$  can be varied continuously. A model of the NACA 0015 airfoil has been built locally. Data for this section were taken from

NACA's lists of wings section [8]. Moreover, the Upper and lower static pressure taps coordinate has been listed in Table 1

Table 1 a- Upper static pressure taps coordinate.

Tap no.	1	2	3	4	5	6	7	8	9	10	11	12	13
x/c	0.01	0.09	0.15	0.20	0.25	0.33	0.5	0.54	0.61	0.66	0.73	0.83	0.95

Tap no.	14	15	16	17	18	19	20
x/c	0.01	0.13	0.24	0.35	0.48	0.59	0.74

The airfoil is supported at a space of 100mm from leading edge. The location of BFS on the upper

surface wing of 125mm from the leading edge Figure 2.

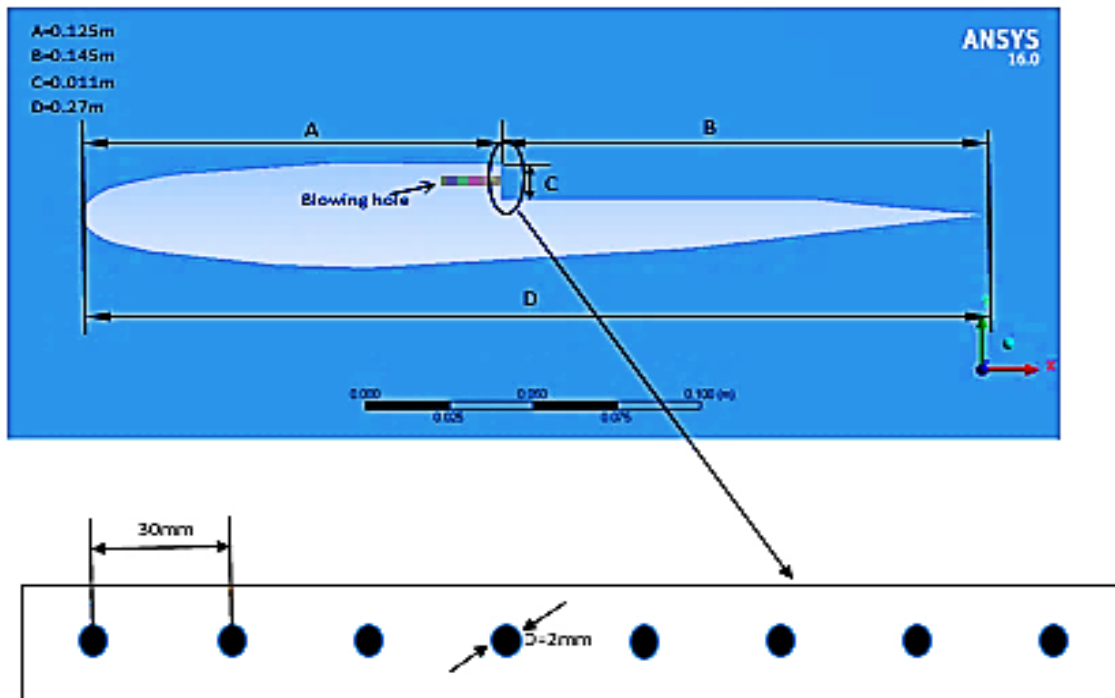


Figure 2: Schematic of Backward-facing step (BFS) airfoil type NACA 0015 with dimension

The blowing system used in present study consists of multi holes, 8 discrete holes with 2mm diameter is distributed along the backward-facing step of the wing. The distance between the first center holes to the neighbor center is 30mm Figure 2. This distribution is used to investigate the effect of blowing method on the characteristics of pressure coefficients ( $C_p$ ) and flow separation over the airfoil. Pressure coefficients have been measured and calculated by using surface pressure measurements technique that uses 13 pressure tapings over the suction surface of the wing. A multiple tube manometer was used to measure the surface pressure distribution.

### 1.1 Calculation of Pressure Coefficient

Many methods used to measure pressure coefficient  $C_p$  on the airfoil. In this work, the pressure coefficient, on the airfoil has been determined from measured pressure distribution over the airfoil's surface. The pressure distribution on the airfoil is expressed in dimensionless form by the pressure coefficient  $C_p$  as follow [10]:

$$c_p = \frac{p_o - p_\infty}{0.5\rho U_\infty^2} \quad (1)$$

Where  $P_o$  is the surface pressure measured at position  $i$  on the surface,  $P_\infty$  is the pressure in the free stream,  $\rho$  is air density, and  $U_\infty$  is the free-stream velocity known by:

$$U_\infty = \sqrt{\frac{2(P_{stagnation} - P_\infty)}{\rho}} \quad (2)$$

### 1.2 Numerical Methodology

The CFD was the method of choice in the design of many aerospace, automotive and industrial components and processes in which fluid or gas flows play an important role. These programs can give results as close as the experimental methods. ANSYS Fluent software version 16.0 was used as a tool to design sections in the present study and to show the effect of control flow separation over backward-facing step (BFS) airfoil type NACA 0015 by blowing method. The steady flow field about airfoil with (BFS) has been simulated numerically by resolving the incompressible two-dimensional, Navier-Stokes equations on unstructured grids domain of complex shape. The simulated flow fields (Laminar model) are used to discuss the mechanisms of flow separation, and to explain the differences in separating performance between baseline case and active flow control using blowing technique. The procedures work are import the co-ordinates vertices (texts file to create the curve) of the airfoil [8] in design modeler. The dimensions of the sketches are coinciding to the experimental airfoil with backward-facing step located at 44.4%  $c$  from leading edge. The grids utilized in this work are unstructured triangles grids and to ensure the computed aerodynamic results are independent of the size of the grid, the density of the grid increased until an insignificant difference was reached in the solution towards convergence

(three different meshes are tested). The outside boundary is of a C-topology type with front arc radius of  $12.5c$  and wake distance of  $20c$ . Create the geometry for the C-mesh domain by using sketcher toolbox and dimension tool. The mesh is constructed fine for the region of the boundary layer near the airfoil surface and coarser away from the airfoil (number of elements 50000). The surface edges of the upper airfoil have 50

divisions before and after the BFS up to (T.E.). Otherwise, BFS edge is divided into 10 divisions. The mesh boundaries were given set to the x and y velocity components, and the end boundary the property “pressure-outlet” to simulate the zero gauge pressure. The airfoil itself is given as wall properties. The Setting boundary conditions as shown in Table 2.

Table 2 Operating parameters.

INPUT	VALUE	INPUT	VALUE
Velocity of flow	25 m/s	Density of fluid	1.225 kg/m <sup>3</sup>
Operating temperature	300 k	Kinematic viscosity	1.5111 × E-5 m <sup>2</sup> /s
Operating pressure	101325 pa	Angle of attack	0° to 20°
Models	Laminar	Fluid	Air

The Reynolds number is specified as low sufficient to simulate an incompressible flow for comparison with experimental data. The Reynolds number is fixed at  $Re=4.4 \times 10^5$  as in the experiments and numerical literature based on the airfoil chord and free stream velocity. The initial condition for all calculations is a free-flow condition and the calculations continue until the periodic vortex shedding is reached. Experimental results of pressure distribution for the (BFS) airfoil at angles of attack  $\alpha = 0^\circ, 5^\circ, 10^\circ, 12^\circ, 14^\circ, 16^\circ$  without blowing and they are compared with blowing Figures 3 & 4. Numerical results of pressure distribution, has been illustrated as shown in Figure 5,6,7,8,9,10,11,12 & 13.

1. Result and Discussion

Figure 3 show experimental results of the distribution of pressure coefficient  $C_p$  on the upper surface Backward-facing step (BFS) airfoil type NACA 0015 with changes the angle of attack without blowing. At the beginning of the airfoil, Peak pressure shows the normal behavior of the pressure curve due to the acceleration of the flow. At the backward-facing step location the pressure coefficient distributions curve shows a decrease in the pressure value due to the sudden change in velocity (passive) and then increases over time due to the slow flow.

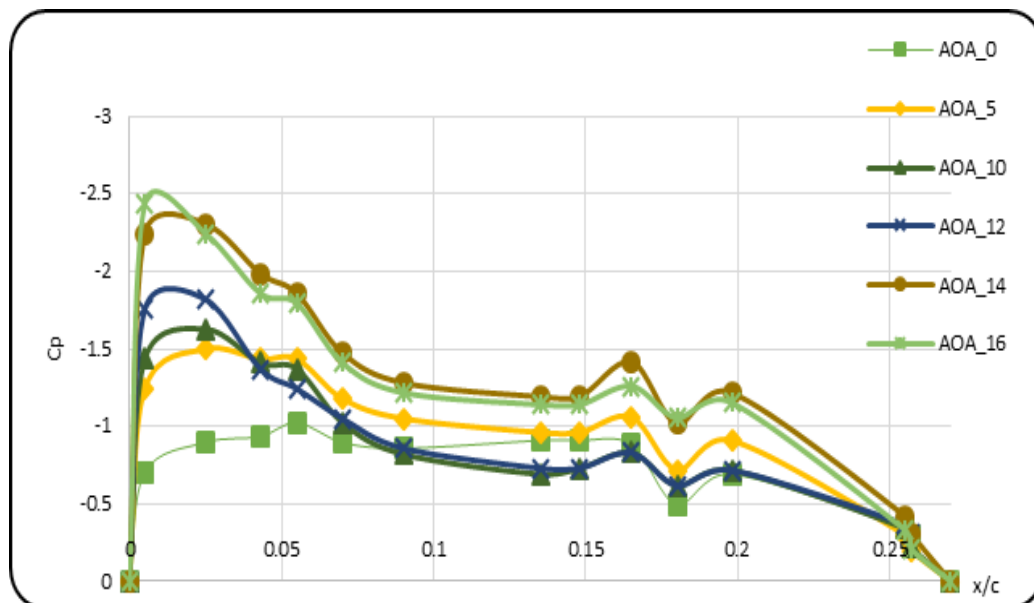


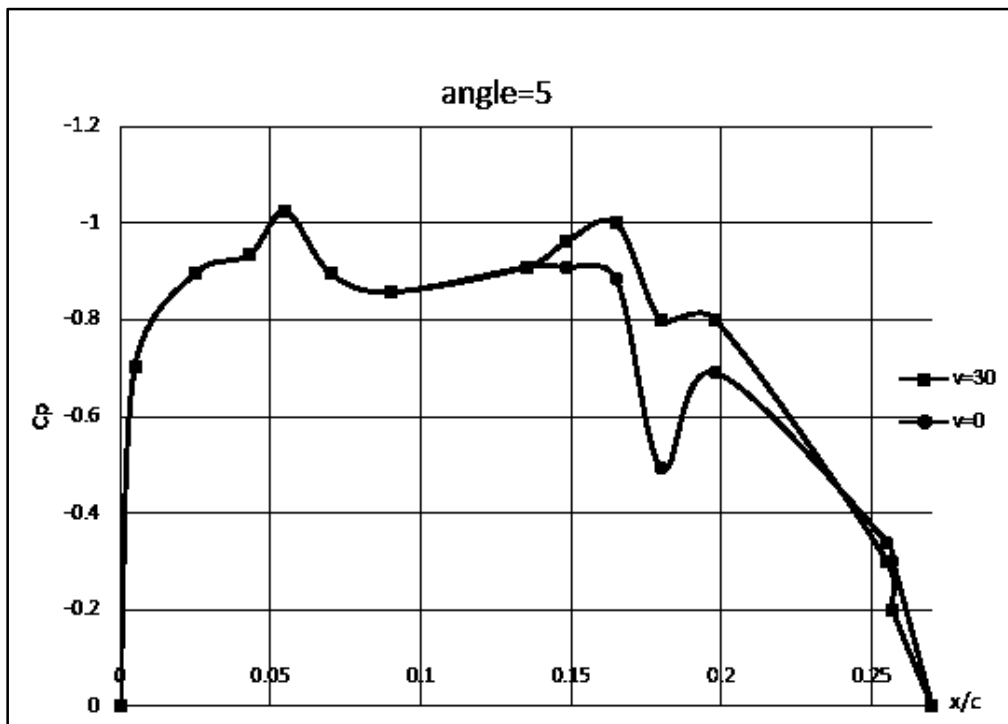
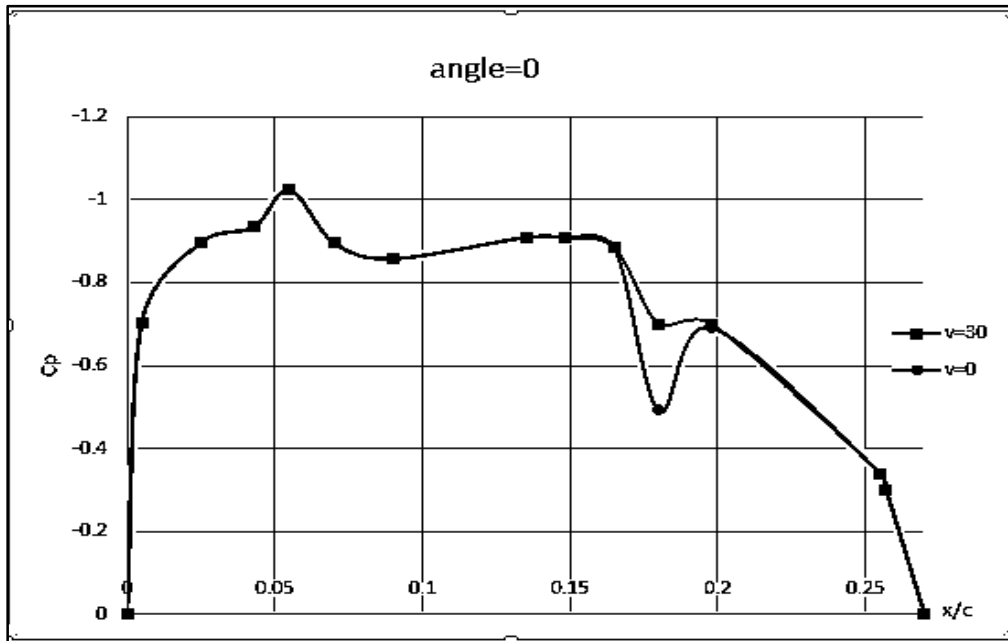
Figure 3: Pressure coefficient distributions  $C_p$  on the upper surface Backward-facing step (BFS) airfoil type NACA 0015 with changes the angle of attack without blowing

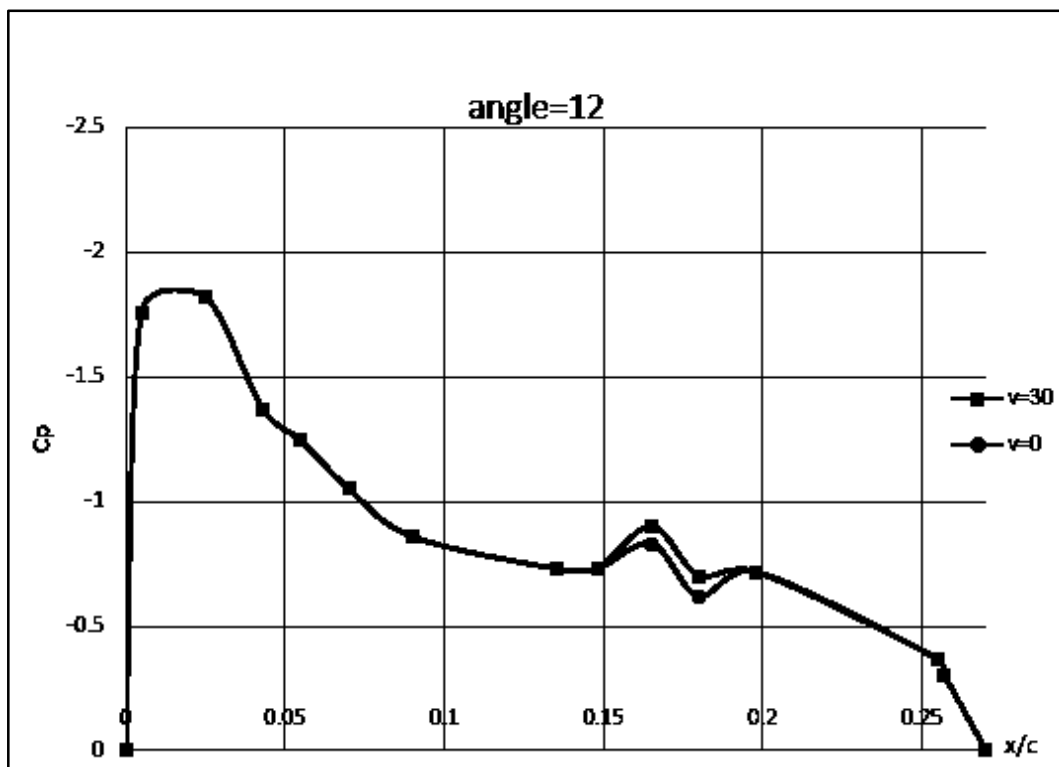
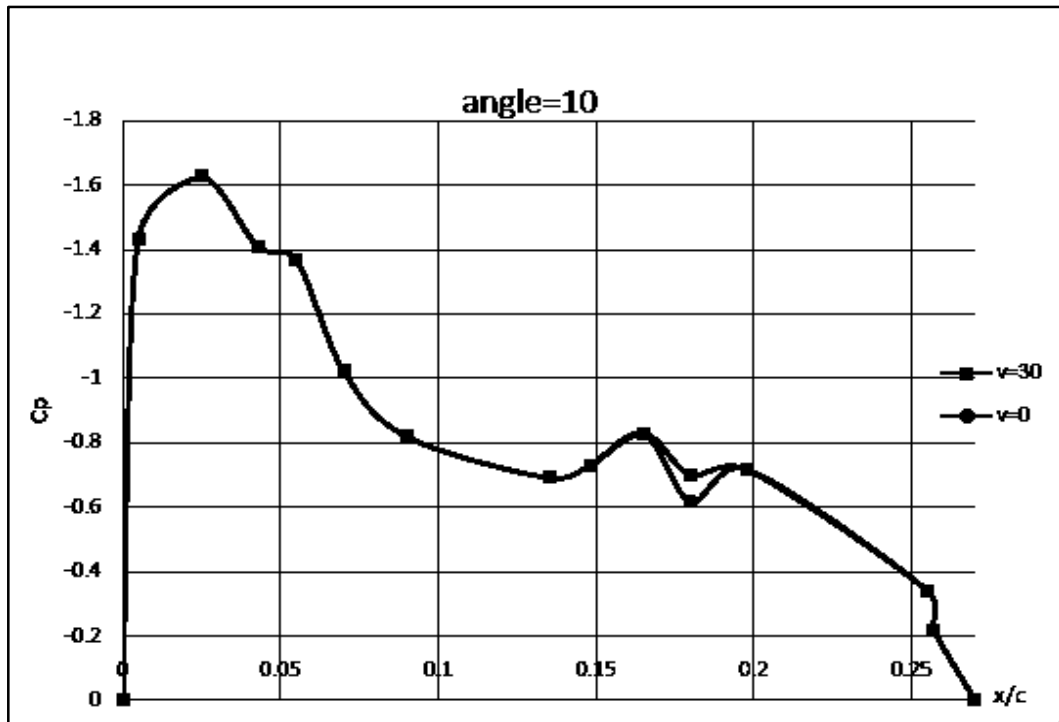
Figure 4 illustrated the comparison between the experimental results of the pressure coefficient on

the upper surface of the airfoil before and after using the blowing technique at a blowing velocity

30m/s with various angles of attack of  $0^\circ < \text{AOA} < 16^\circ$ . The change in the pressure coefficient is noticeable when using the technique especially at the location of the excitation (44.4% c from leading edge). As shown in the figure, blowing

technique is most effective at small angles of attack ( $0^\circ, 5^\circ$ ) and less influence at the angle of attack  $10^\circ$  and more because the blowing velocity is relatively parallel to the flow velocity which give more momentum to flow.





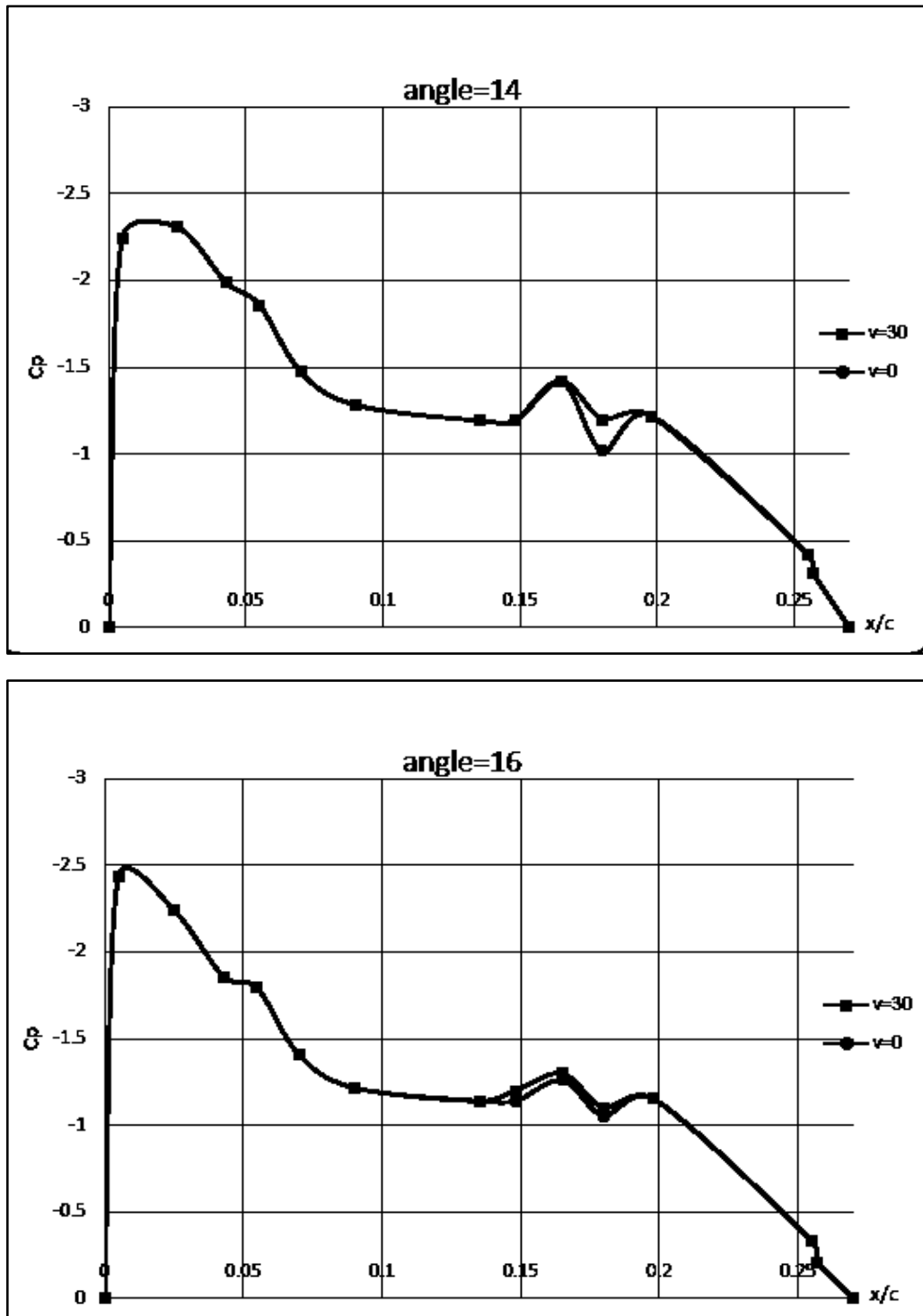


Figure 4: Pressure coefficient distributions  $C_p$  on the upper surface Backward-facing step (BFS) airfoil type NACA 0015 with changes the angle of attack with blowing speed  $v = 30\text{m/s}$

Figure 5-a shows the pressure coefficient distributions measurements around the NACA 0015 airfoil at the angle of attack 0 deg captured

from ANSYS Fluent. For a 0 deg angle of attack the points on the both upper and lower surfaces almost match exactly, because of the symmetry airfoil.



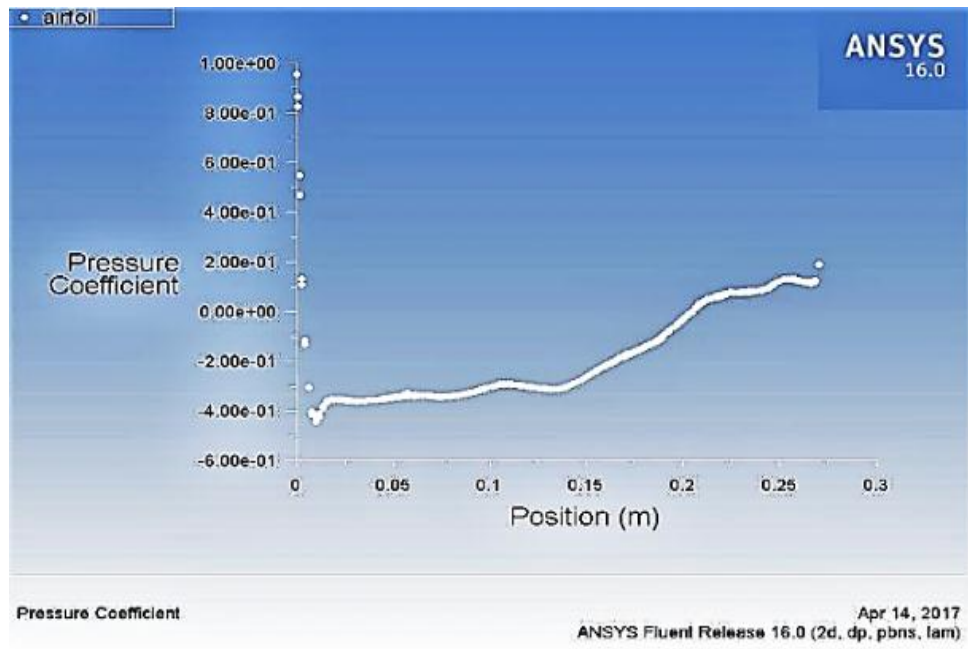


Figure 5-a: Pressure Coefficient Distributions around the NACA 0015 airfoil at the angle of attack 0 deg captured from ANSYS Fluent

From the velocity contours shown in the Figure (5-b) taken from ANSYS Fluent, velocity vector plots with angle of attack 0 deg for the NACA 0015 airfoil without BFS. The laminar flow

remains attached the airfoil suction surface area and leaves the airfoil surface smoothly without separation flow.

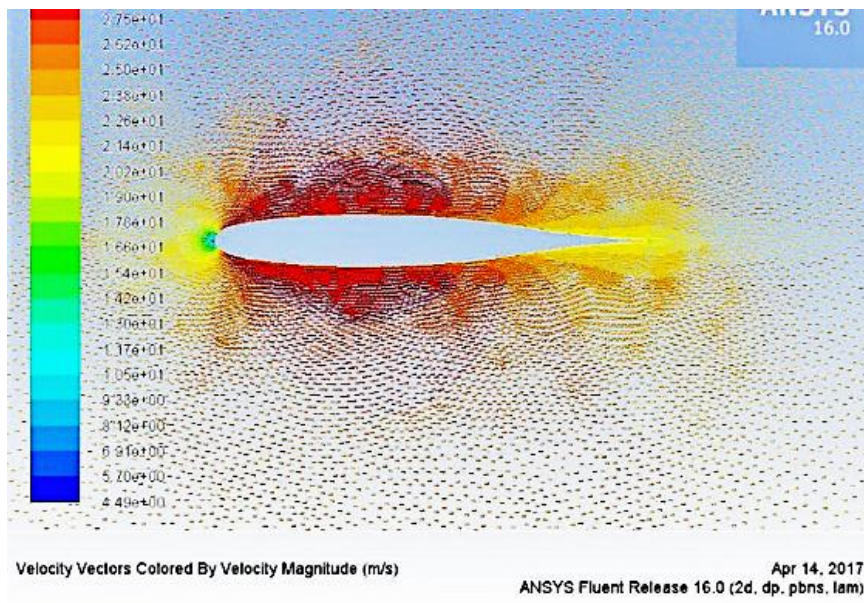
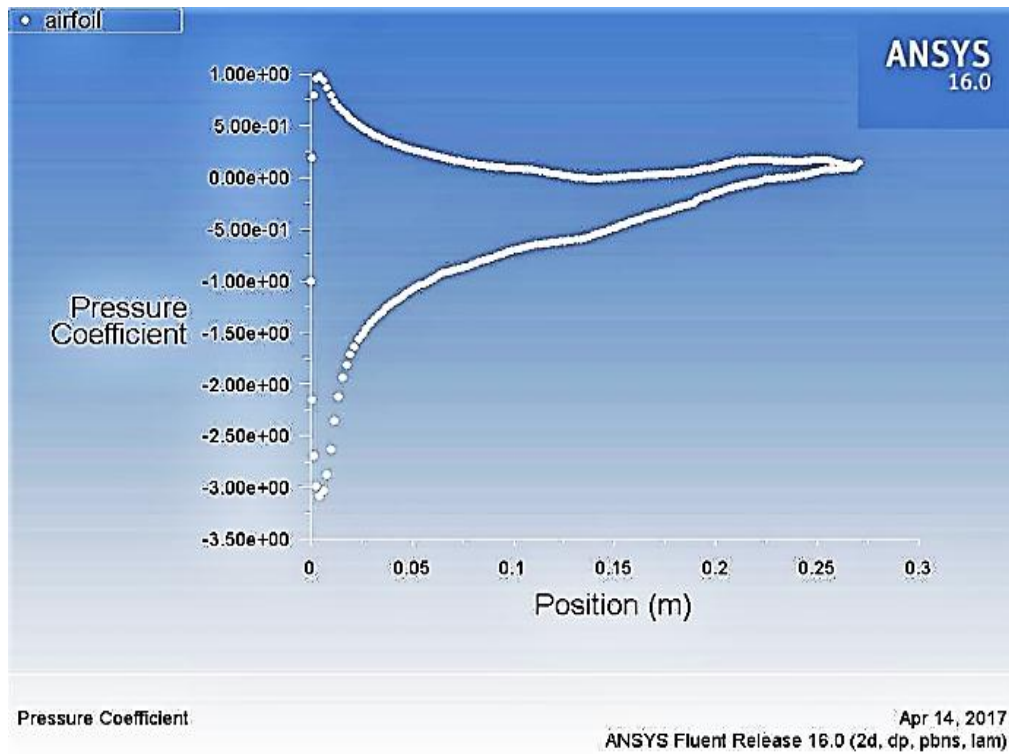


Figure 5-b: Velocity Vectors around the NACA 0015 airfoil at the angle of attack 0 deg captured from ANSYS Fluent

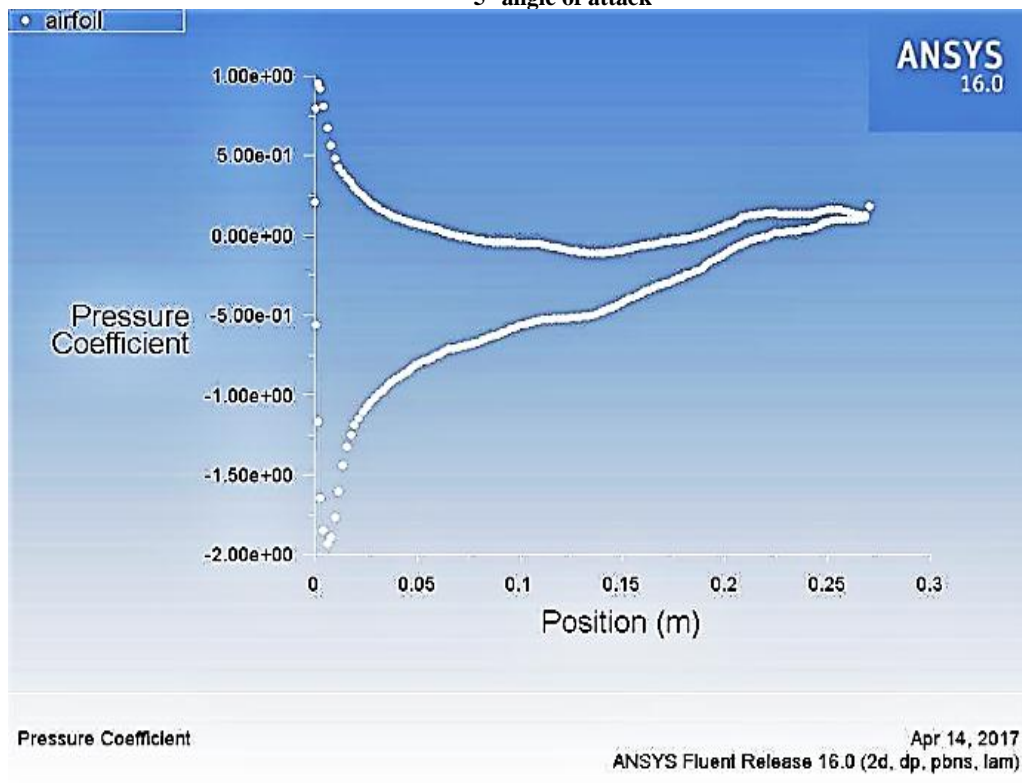
Figure 6 shows the surface pressure coefficient distributions  $C_p$  measured around the airfoil without BFS, since the angle of attack changes from 5.0 deg to 20.0 deg. It was found that the surface pressure distribution on the upper surface of the airfoil varied significantly at different angles of attack\_AOA\_ 5.0 to 14 deg and remains unchanged until angle of attack 20 deg. The surface pressure coefficient profiles along the

upper surface of the airfoil rapidly reach their negative peaks at positions close to the leading edge of the airfoil, the surface pressure is then gradually and smoothly recovered over the upper surface of the airfoil to the trailing edge of the airfoil. After AOA 20 deg the negative peaks decreases at the location near to the airfoil leading edge.

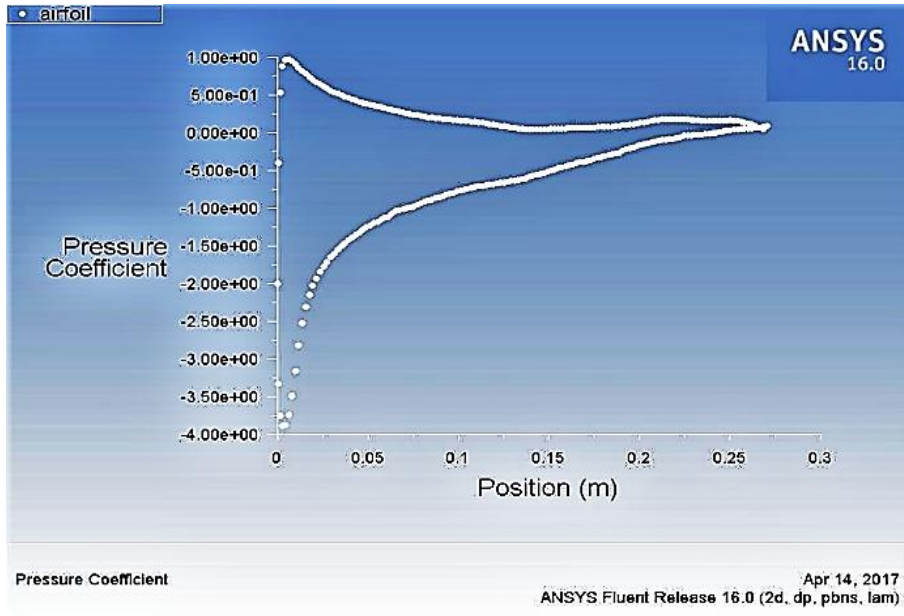




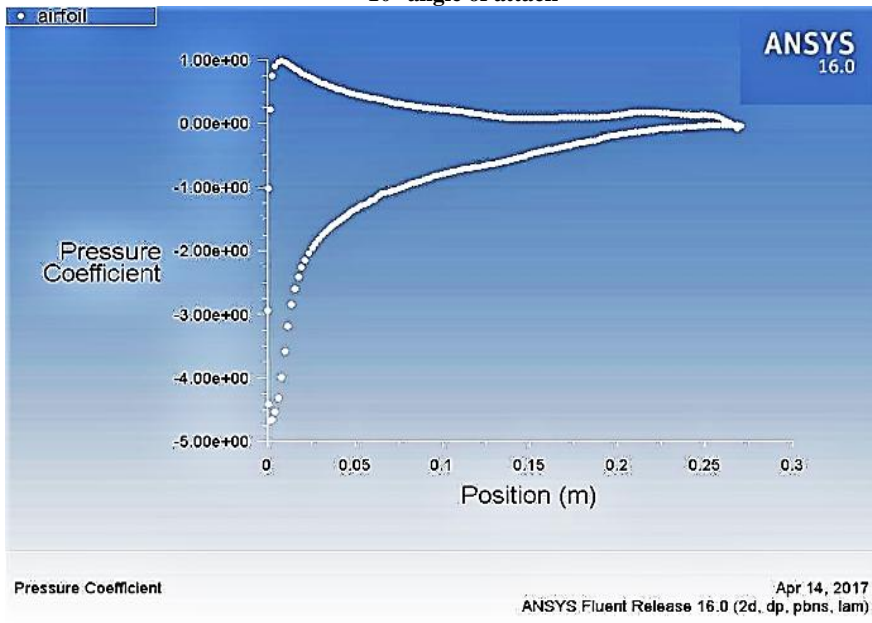
5° angle of attack



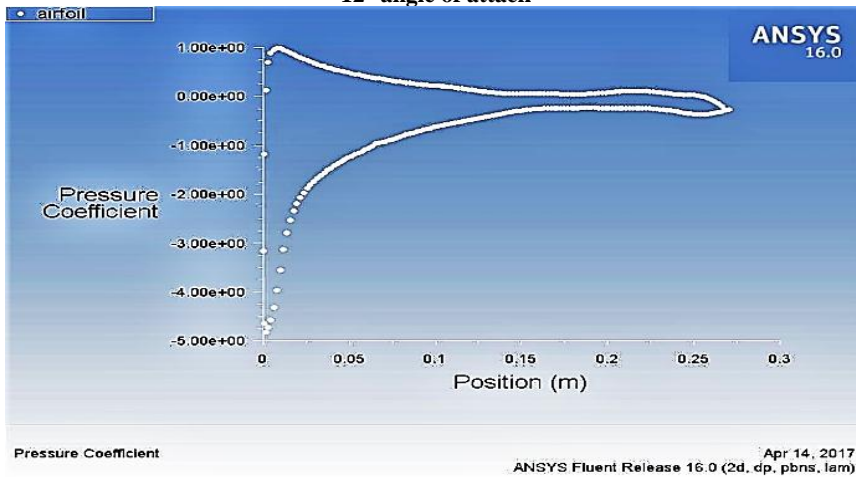
8° angle of attack



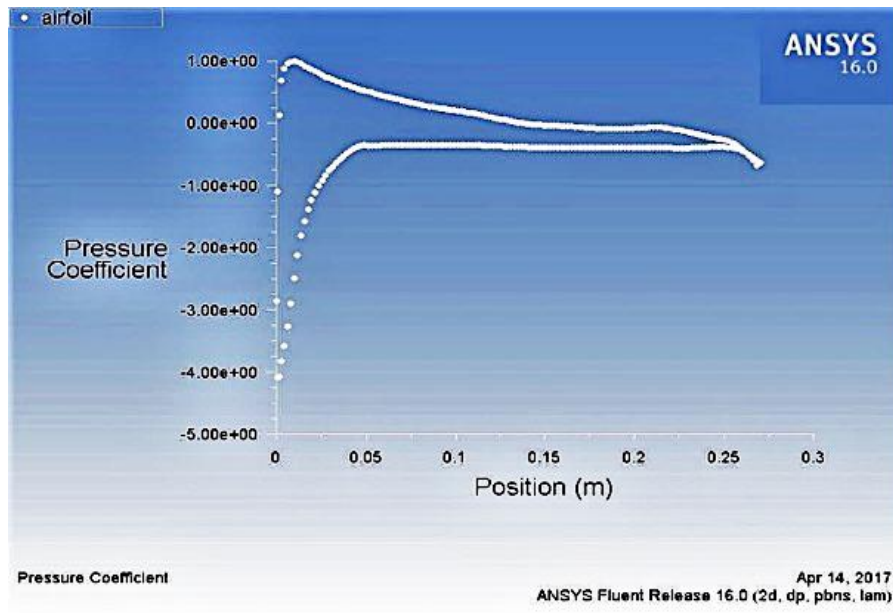
10° angle of attack



12° angle of attack



14° angle of attack

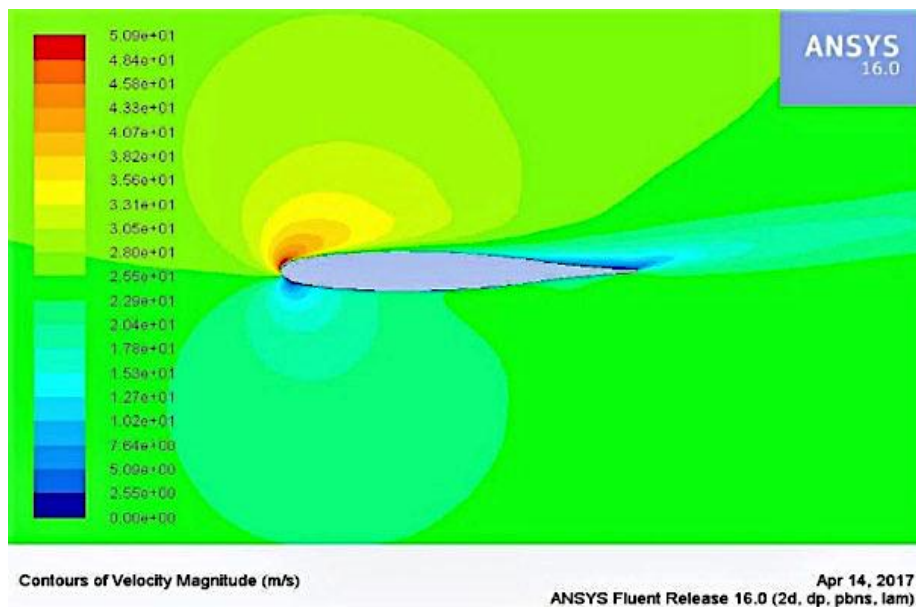


20° angle of attack

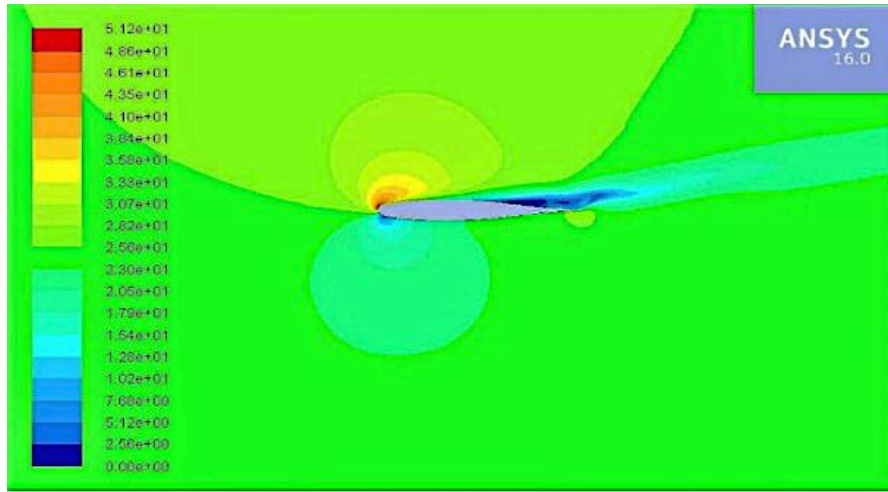
Figure 6: Pressure coefficient distributions  $C_p$  around the airfoil without BFS as the angle of attack changes from 5.0 deg to 20.0 deg

As schematically illustrated in Figure 7, Contours of Velocity Magnitude (m/s) shows the separation point (The velocity in the wall is zero or negative and there is a point of inflection in the velocity profile and a positive or negative pressure

gradient occurs in the direction of the flow) on the surface of the airfoil was found to be displaced upstream to approach the front edge of the airfoil as the AOA increased.

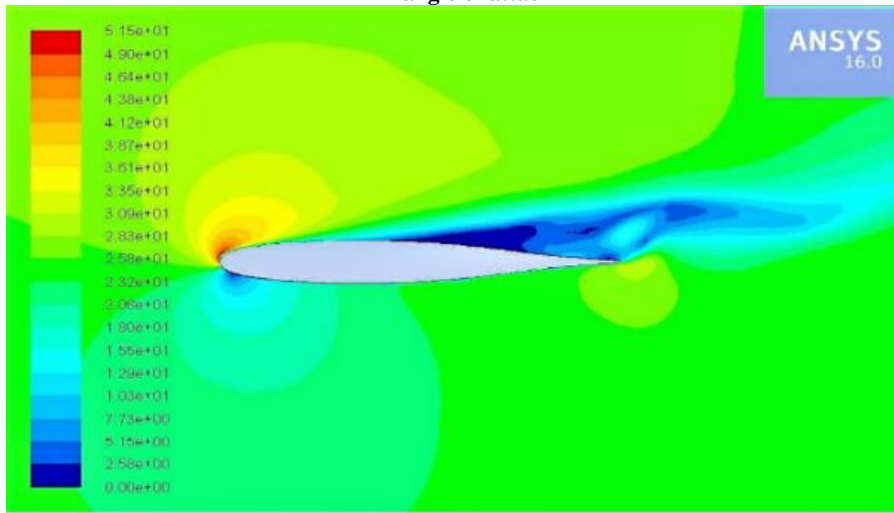


12° angle of attack



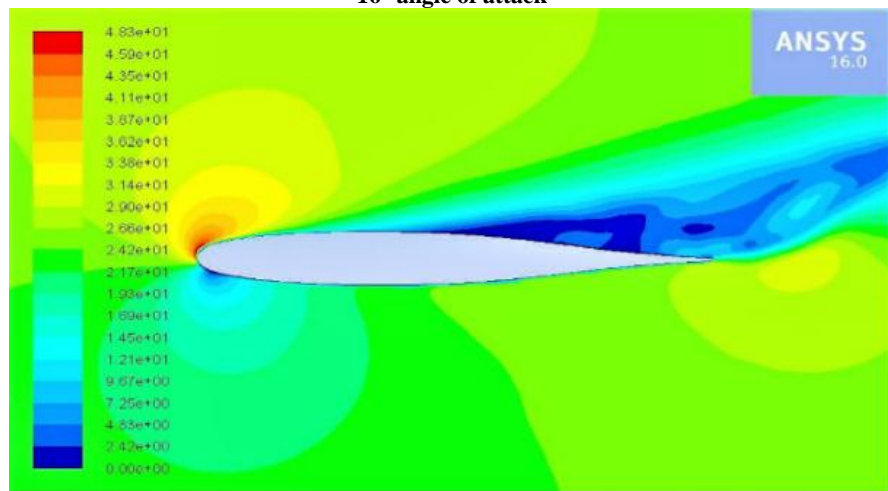
Contours of Velocity Magnitude (m/s) ANSYS Fluent Release 16.0 (2d, dp, pbns, lam) Apr 14, 2017

14° angle of attack



Contours of Velocity Magnitude (m/s) ANSYS Fluent Release 16.0 (2d, dp, pbns, lam) Apr 14, 2017

16° angle of attack



Contours of Velocity Magnitude (m/s) ANSYS Fluent Release 16.0 (2d, dp, pbns, lam) Apr 14, 2017

18° angle of attack

Figure 6:Contours of Velocity Magnitude (m/s) as the angle of attack changes from 12.0 deg to 18.0 deg



The effect of backward-facing step (BFS) airfoil type NACA 0015 on the surface pressure coefficient profiles along the upper surface of airfoil at 0° angle of attack was shown in Fig (8).

As illustrated in Fig(8-b) there is a clear improvement in pressure coefficient curve compare with the airfoil without BFS as in fig(8-a).

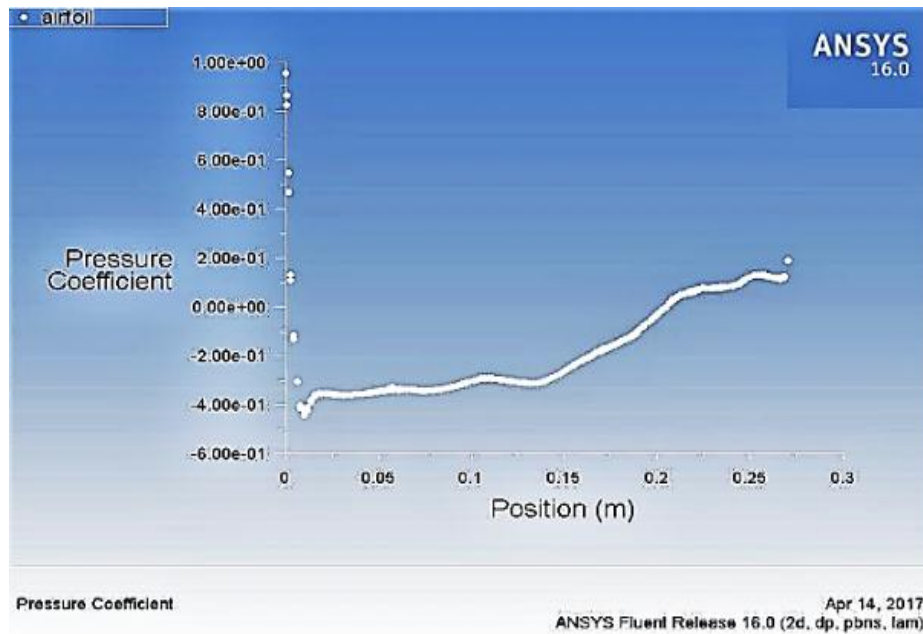


Figure 8-a: Pressure Coefficient Distributions around the NACA 0015 airfoil without BFS at the angle of attack 0 deg captured from ANSYS Fluent

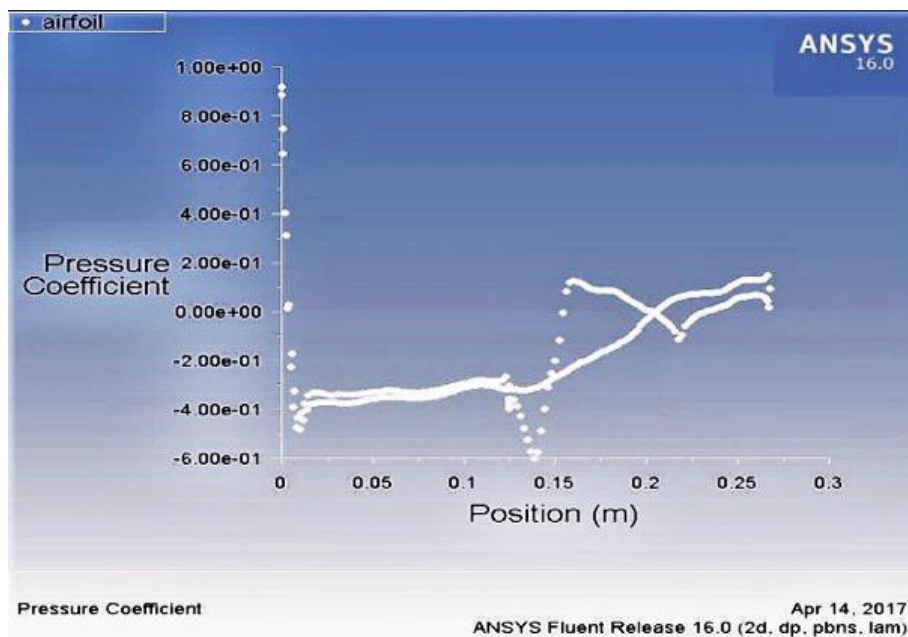
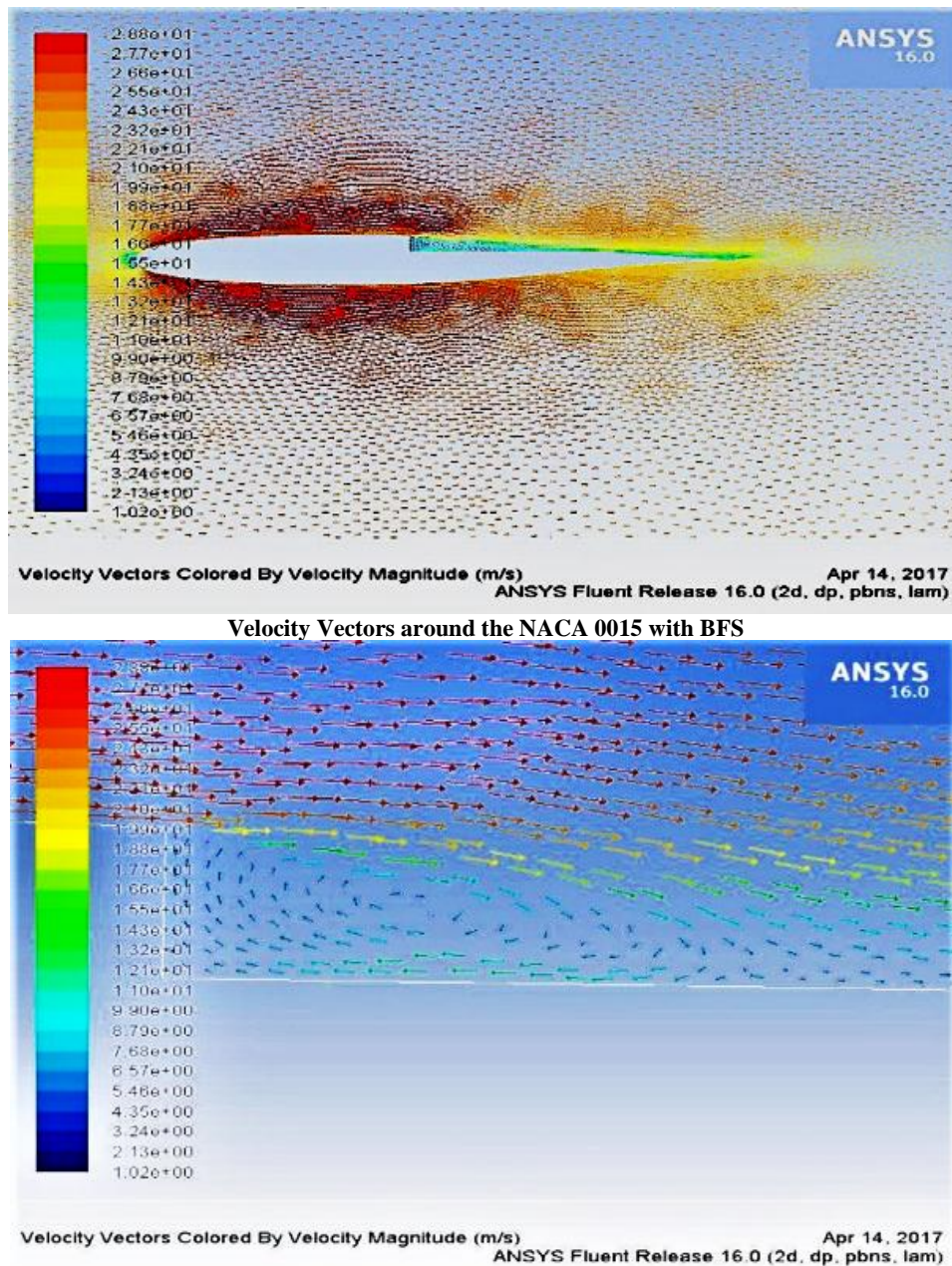


Figure 8-a: Pressure Coefficient Distributions around the NACA 0015 airfoil with BFS at the angle of attack 0 deg captured from ANSYS Fluent

As a result of a change in velocity of the flow layer near the surface of the airfoil due to the transformation of the laminar flow to turbulence at the location backward-facing step as shown in fig(9) .it shows that the velocity of the air is slower at the backward facing-step region compared to the lower surface of the airfoil.

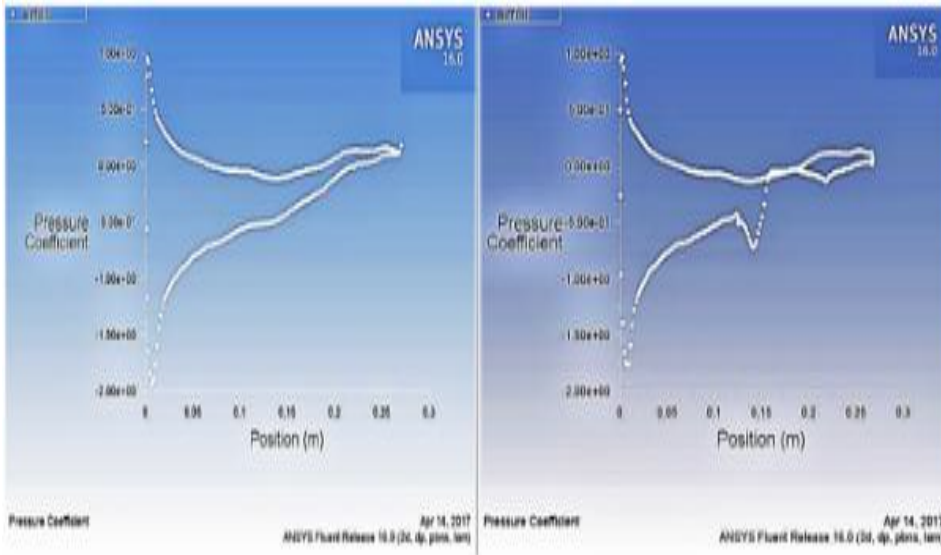
Additionally, a clockwise direction vortex can be observed in the backward facing step region generating lift [9]. Sharp corner cause the boundary layer flow unable to turn (that's acceleration should increase rapidly), making recirculation in the aft region of the backward facing step and separation at the edge.



**Figure 9: Behavior of the flow and a clockwise direction vortex can be observed in the backward facing step region generating at BFS (Velocity Vectors by velocity magnitude captured from ANSYS Fluent at angle of attack 0 deg)**

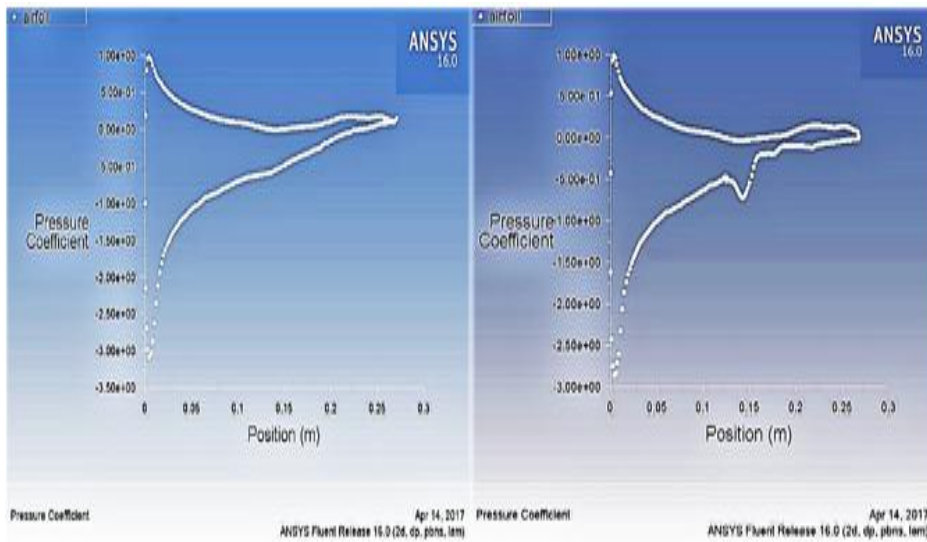
Figure 10 by comparing the pressure coefficient profiles without the backward facing step and with it at different angles of attack (5°-14°) notice increase in the area under curve to pressure

coefficient for backward-facing step airfoil. This increase is evident at the angles of attack 5, 8, 10 deg and improved slightly at the angle of attack 12deg.



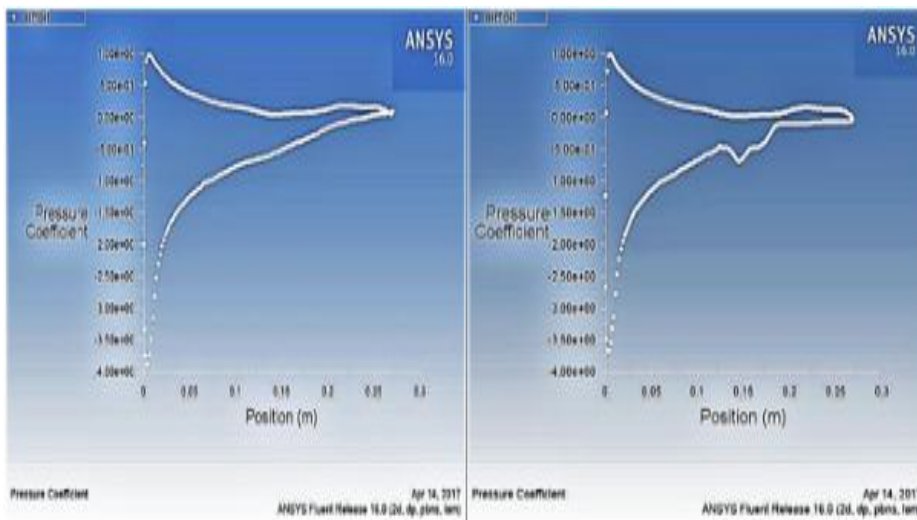
5° angle of attack Without BFS.

5° angle of attack With BFS.



8° angle of attack Without BFS.

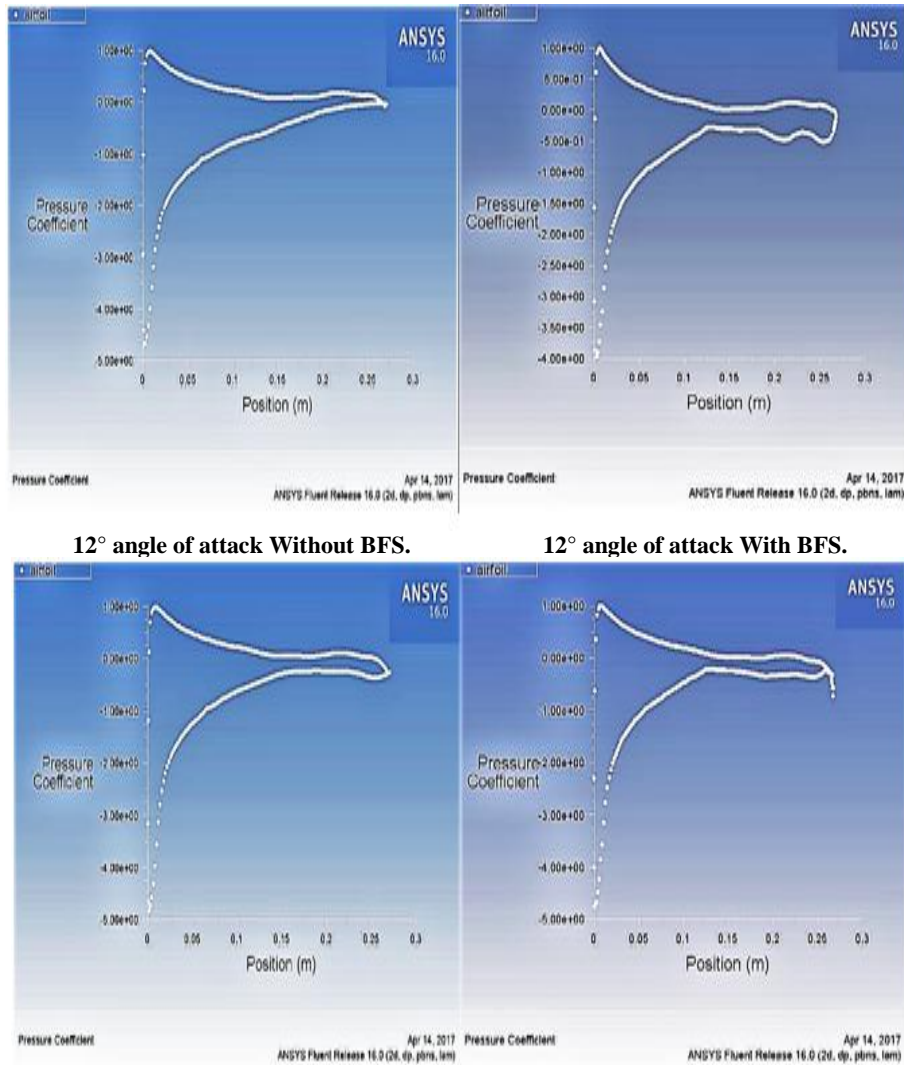
8° angle of attack With BFS.



10° angle of attack Without BFS.

10° angle of attack With BFS.





12° angle of attack Without BFS.

12° angle of attack With BFS.

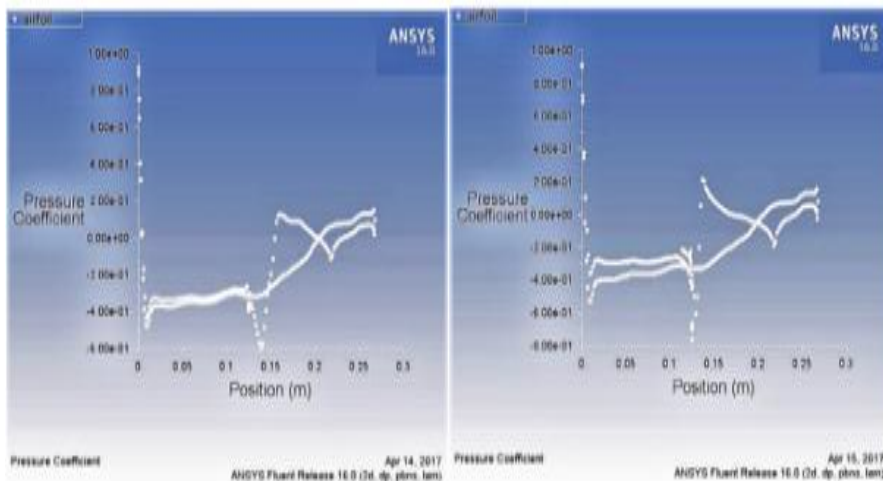
14° angle of attack Without BFS.

14° angle of attack With BFS.

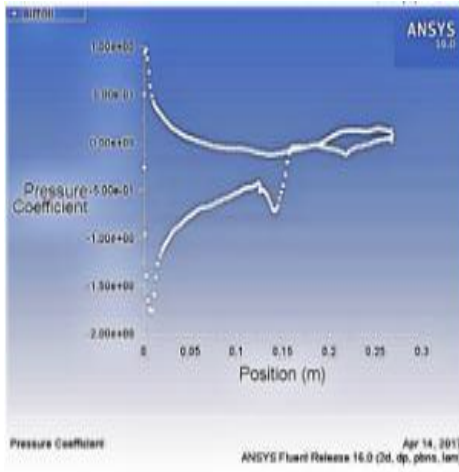
Figure 10: Comparing the pressure coefficient profiles with and without the backward facing step for NACA 0015

The effect of employing a backward-facing step airfoil with blowing at velocity 30m/s on the suction side of a National Advisory Committee for Aeronautics (NACA) 0015 airfoil at Reynolds

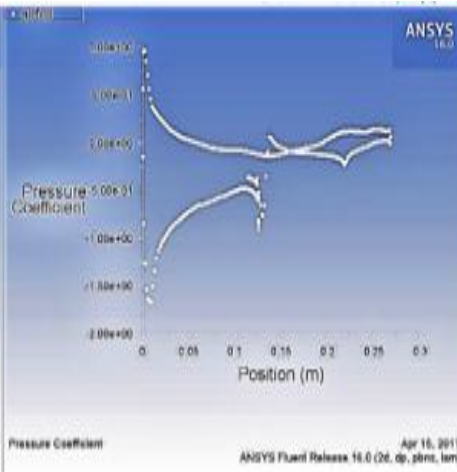
number of  $(4.4 \times 10^5)$  was observed Figure 11. However, these BFS with blowing effects are shifting the separation point location towards the trailing edge.



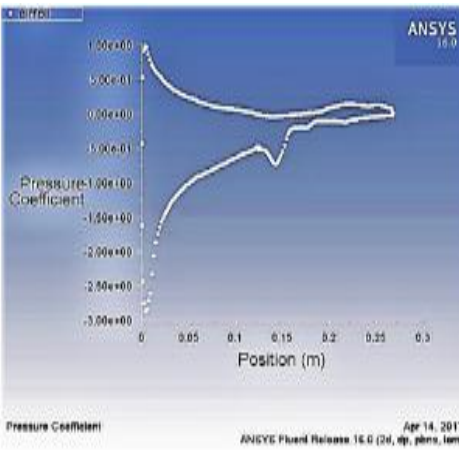
**BFS without blowing ( $\alpha=0^\circ$ ).**



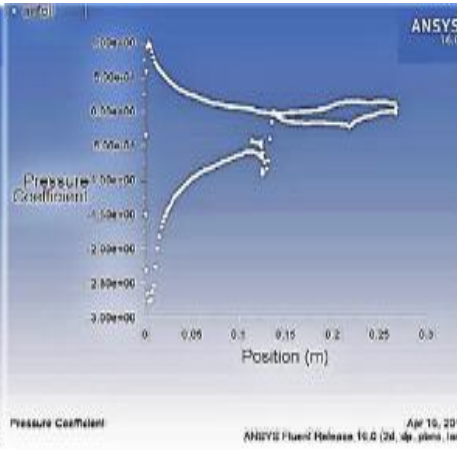
**BFS with blowing ( $\alpha=0^\circ$ ).**



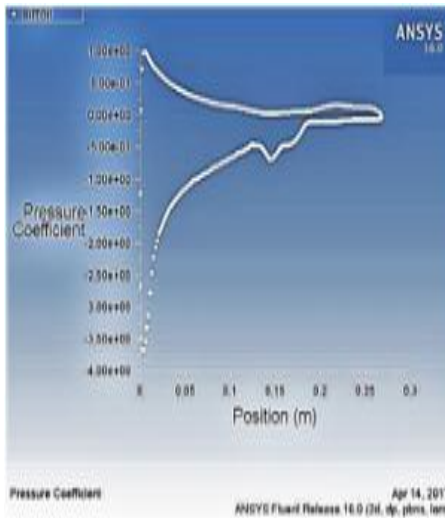
**BFS without blowing ( $\alpha=5^\circ$ ).**



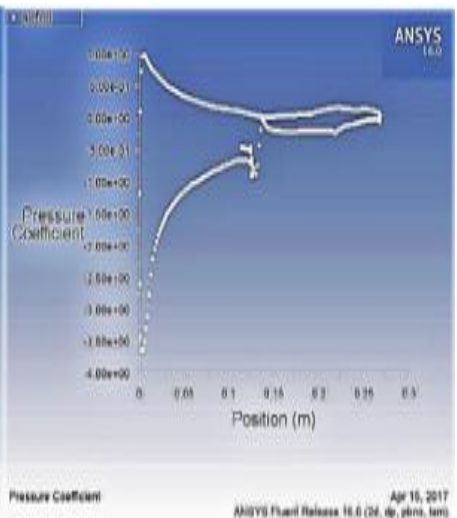
**BFS with blowing ( $\alpha=5^\circ$ ).**



**BFS without blowing ( $\alpha=8^\circ$ ).**



**BFS with blowing ( $\alpha=8^\circ$ ).**

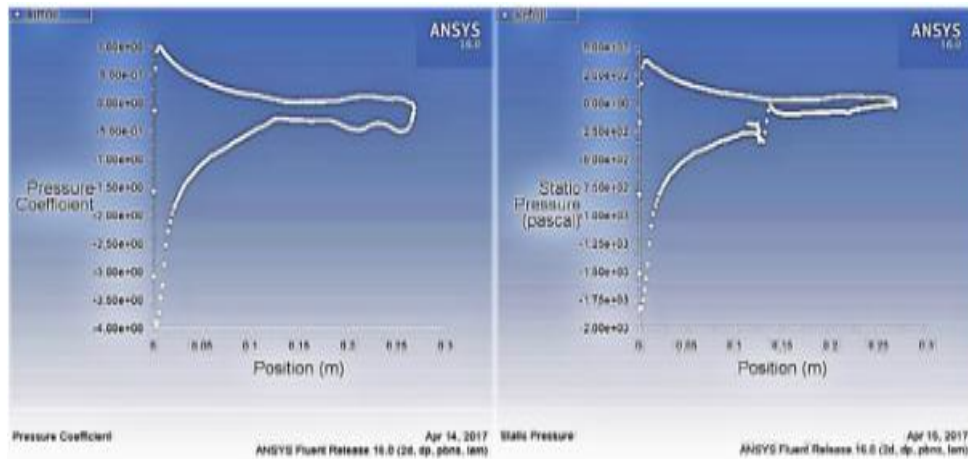


**BFS without blowing ( $\alpha=10^\circ$ ).**



**BFS with blowing ( $\alpha=10^\circ$ ).**





**BFS without blowing ( $\alpha=12^\circ$ ).      BFS with blowing ( $\alpha=12^\circ$ ).**  
**Figure 11: Comparing the pressure coefficient profiles without and with blowing to backward facing step for NACA 0015**

By comparing the pressure coefficient and velocity vectors colored by velocity magnitude (m/s) at  $0^\circ$  angle of attack as in Figure 12-a for airfoil without BFS, Figure 12-b with BFS without blowing, Figure 12-c BFS with single

blowing technique and Figure 12-d BFS airfoil with multiple blowing technique, Note the change in the pressure coefficient curve when using blowing technique.

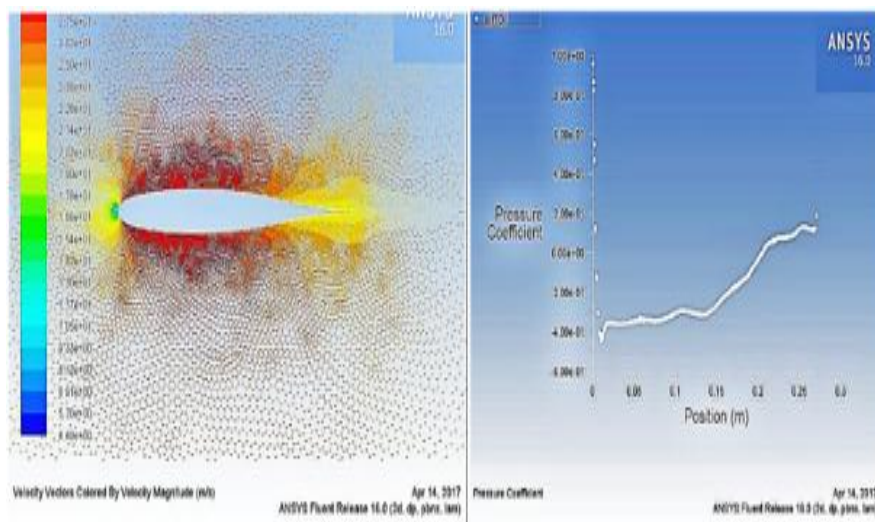


**Figure 12-a: pressure coefficient for NACA 0015 at angle of attack 0 deg**

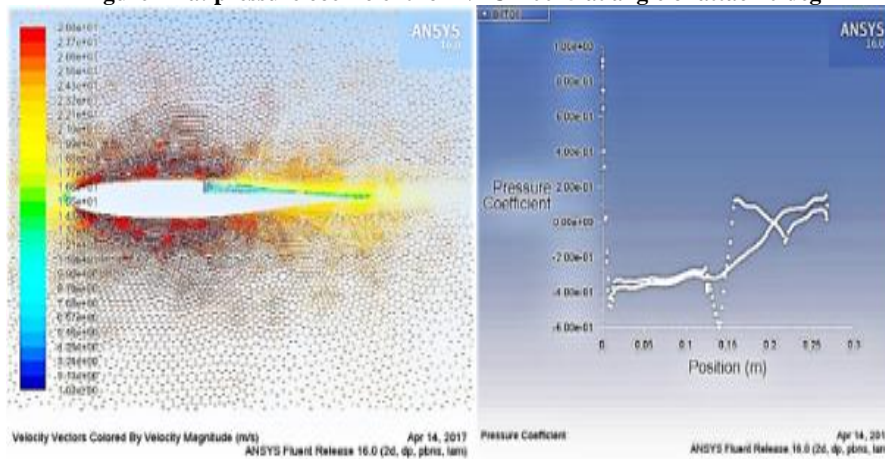


**Figure 12-b: pressure coefficient profiles without blowing to backward facing step for NACA 0015 at angle of attack 0 deg**



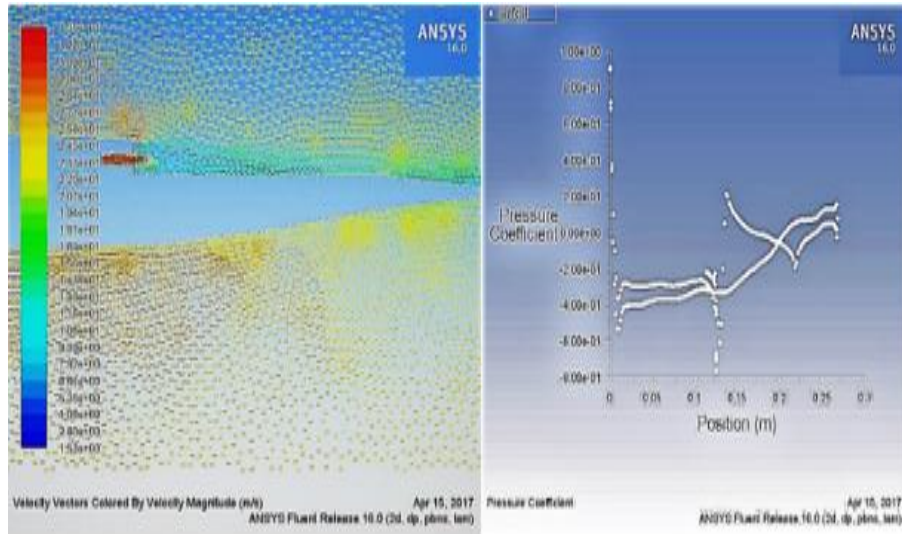


Figure 12-c: pressure coefficient profiles with single blowing to backward facing step for NACA 0015 at angle of attack 0 deg

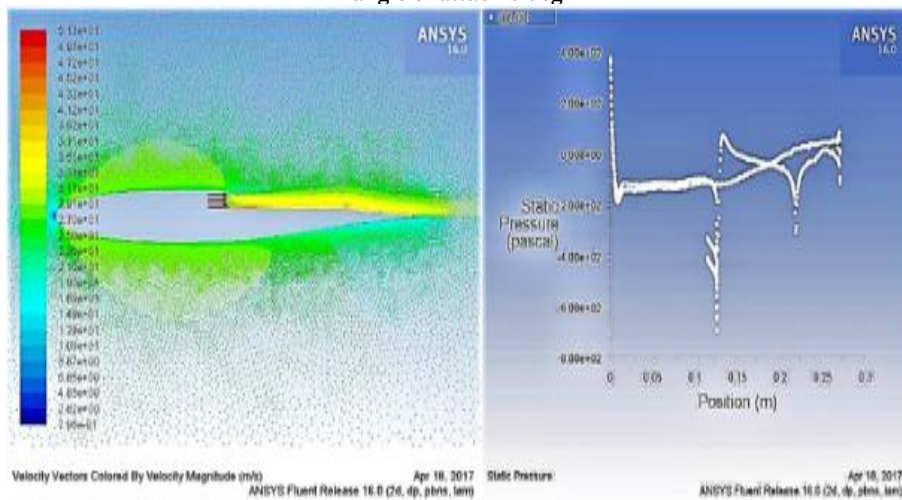
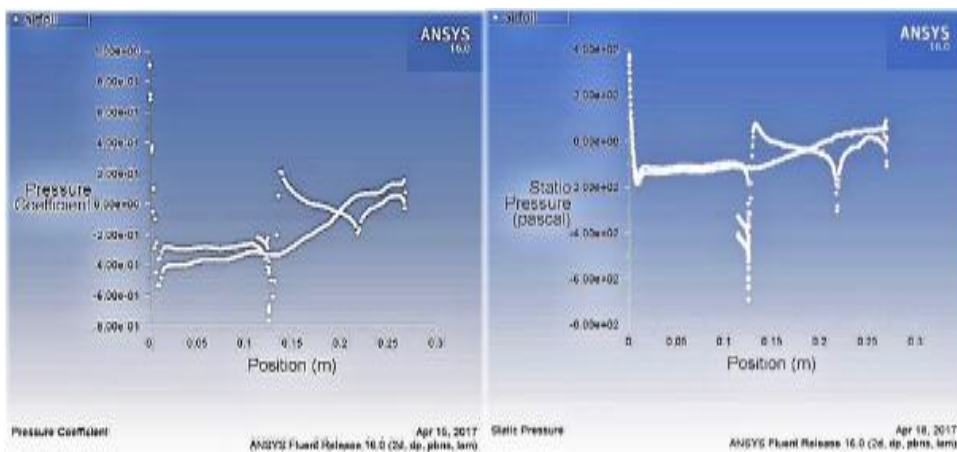


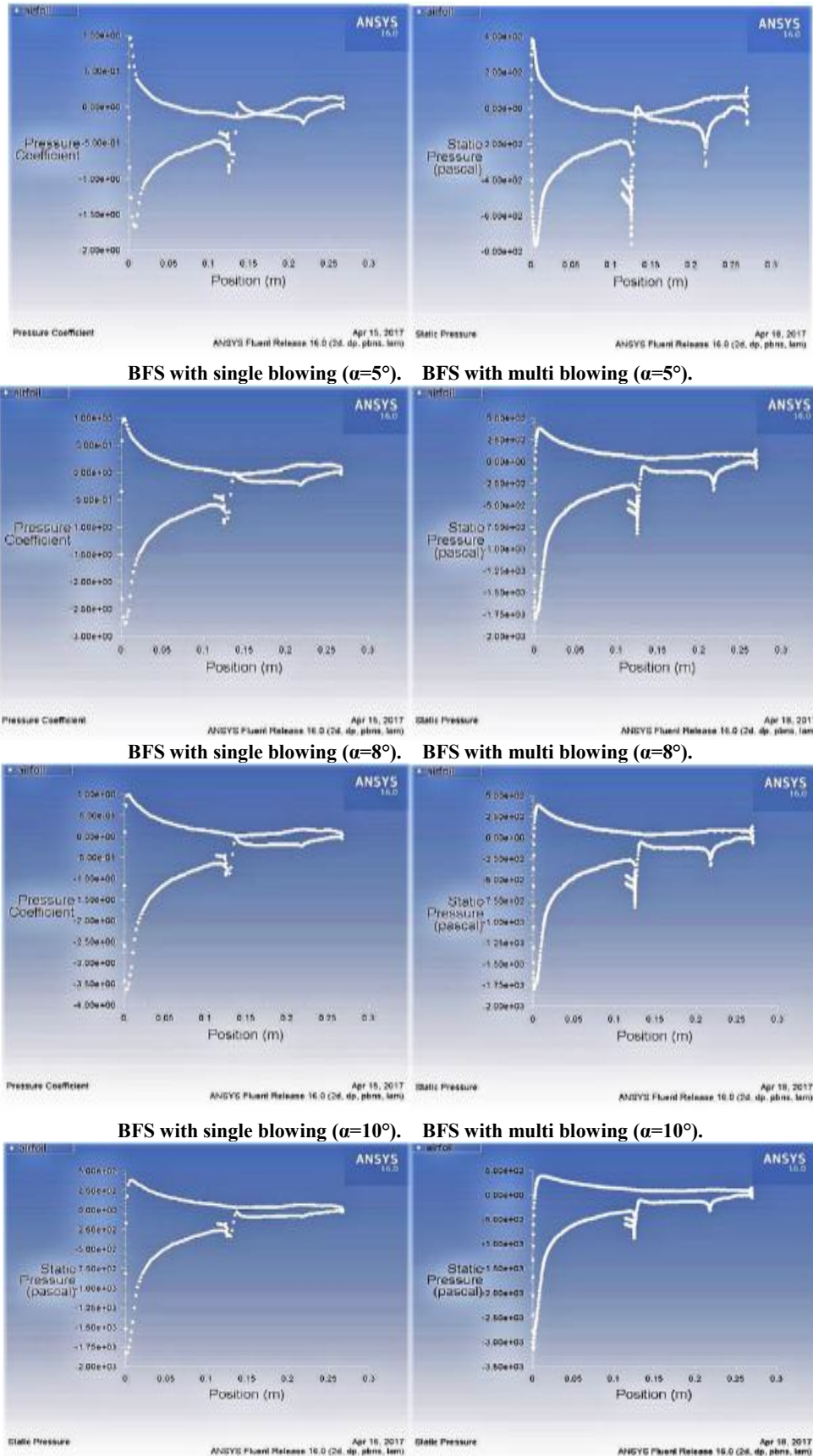
Figure 12-d: pressure coefficient profiles with multiple blowing to backward facing step for NACA 0015 at angle of attack 0 deg

For backward-facing step (BFS) airfoil, using a multi-hole blowing technique with blowing velocity 30 m / s and comparing it with the same

technique have single hole there is same change in the coefficient of the pressure as noted in Figure 13.



BFS with single blowing ( $\alpha=0^\circ$ ). BFS with multi blowing ( $\alpha=0^\circ$ ).



**BFS with single blowing ( $\alpha=5^\circ$ ). BFS with multi blowing ( $\alpha=5^\circ$ ).**

**BFS with single blowing ( $\alpha=8^\circ$ ). BFS with multi blowing ( $\alpha=8^\circ$ ).**

**BFS with single blowing ( $\alpha=10^\circ$ ). BFS with multi blowing ( $\alpha=10^\circ$ ).**

**BFS with single blowing ( $\alpha=12^\circ$ ). BFS with multi blowing ( $\alpha=12^\circ$ ).**

**Figure 13: Comparing the pressure coefficient profiles with single and with multi blowing to backward facing step for NACA 0015**

## 2. Conclusion

- 1-An improvement in the pressure coefficient for backward-facing step (BFS) airfoil using blowing technique.
- 2-For the experimental results, the change in the pressure coefficient is noticeable when using the blowing technique especially at the location of the excitation (44.4% c) from leading edge.
- 3-Blowing technique is most effective at small angles of attack (0°, 5°, 8°) and less influence at the angle of attack 10° for the experimental study.
- 4-Separation point was delay when using Blowing technique on the backward-facing step (BFS) airfoil.
- 5-There is same change in the coefficient of the pressure when using single and a multi-hole blowing technique with velocity 30 m / s for backward-facing step (BFS) airfoil.

facing step flow, *Journal of Fluids and Structures* 12(6), (1998), p.p 703-716.

- [10]. Houghton, Edward Lewis, and Peter William Carpenter. *Aerodynamics for engineering students*. Butterworth-Heinemann, 2003.

## References

- [1].Tuck, A., and J. Soria., Active flow control over a NACA 0015 airfoil using a ZNMF jet, 15th Australasian fluid mechanics conference. 2004.
- [2].Jansen, D. P., *Passive Flow Separation Control on an Airfoil-Flap Model (The Effect of Cylinders and Vortex Generators)*, 2012.
- [3].Šarić, S., S. Jakirlić, and Cameron Tropea, A periodically perturbed backward-facing step flow by means of LES, DES and T-RANS: an example of flow separation control, *Journal of Fluids Engineering* 127(5), (2005), 879-887.
- [4].Uruba, Václav, Pavel Jonáš, and Oton Mazur, Control of a channel-flow behind a backward-facing step by suction/blowing, *International Journal of Heat and Fluid Flow* 28(4), (2007), 665-672.
- [5].Mishriky, Fadi, and Paul Walsh, Effect of the Backward-Facing Step Location on the Aerodynamics of a Morphing Wing, *Aerospace* 3(3), (2016), p.p 25.
- [6].Hasan, M. A. Z., The flow over a backward-facing step under controlled perturbation:laminar separation, *Journal of Fluid Mechanics* 238, (1992), p.p 73-96.
- [7].Chun, Kyung-Bin, and H. J. Sung, Control of turbulent separated flow over a backward-facing step by local forcing, *Experiments in Fluids* 21(6), (1996), p.p 417-426.
- [8].I. H. Abbott & A. E. Van Doenhoff, *Theory of wing Section*, McGraw-Hill ,NY. 1959
- [9].Lee, T., and D. Mateescu, Experimental and numerical investigation of 2-D backward-